Physics Letters B 797 (2019) 134863

Contents lists available at ScienceDirect

Physics Letters B

www.elsevier.com/locate/physletb

Essential elements for nuclear binding

Bing-Nan Lu [a], Ning Li [a], Serdar Elhatisari [b,c], Dean Lee [a,*], Evgeny Epelbaum [d], Ulf-G. Meißner [b,e,f]

[a] *Facility for Rare Isotope Beams and Department of Physics and Astronomy, Michigan State University, MI 48824, USA*
[b] *Helmholtz-Institut für Strahlen- und Kernphysik and Bethe Center for Theoretical Physics, Universität Bonn, D-53115 Bonn, Germany*
[c] *Faculty of Engineering, Karamanoglu Mehmetbey University, Karaman 70100, Turkey*
[d] *Ruhr University Bochum, Faculty of Physics and Astronomy, Institute for Theoretical Physics II, D-44870 Bochum, Germany*
[e] *Institute for Advanced Simulation, Institut für Kernphysik, and Jülich Center for Hadron Physics, Forschungszentrum Jülich, D-52425 Jülich, Germany*
[f] *Tbilisi State University, 0186 Tbilisi, Georgia*

ARTICLE INFO

Article history:
Received 24 May 2019
Received in revised form 11 August 2019
Accepted 14 August 2019
Available online 19 August 2019
Editor: W. Haxton

ABSTRACT

How does nuclear binding emerge from first principles? Our current best understanding of nuclear forces is based on a systematic low-energy expansion called chiral effective field theory. However, recent *ab initio* calculations of nuclear structure have found that not all chiral effective field theory interactions give accurate predictions with increasing nuclear density. In this letter we address the reason for this problem and the first steps toward a solution. Using nuclear lattice simulations, we deduce the minimal nuclear interaction that can reproduce the ground state properties of light nuclei, medium-mass nuclei, and neutron matter simultaneously with no more than a few percent error in the energies and charge radii. We find that only four parameters are needed. With these four parameters one can accurately describe neutron matter up to saturation density and the ground state properties of nuclei up to calcium. Given the absence of sign oscillations in these lattice Monte Carlo simulations and the mild scaling of computational effort scaling with nucleon number, this work provides a pathway to high-quality simulations in the future with as many as one or two hundred nucleons.

Chiral effective field theory (χEFT) is a first principles approach to nuclear forces where interactions are arranged as a low-energy expansion in powers of momentum and pion mass [1,2]. While many calculations establish the reliability of χEFT in describing the properties of light nuclei [3–7], the binding energies and charge radii of medium mass nuclei are not consistently reproduced [5,8–14]. One well-known example is that the charge radius of ^{16}O tends to be too small for most of interactions in the literature [8,10–13]. The core issue is that χEFT many-body calculations do not yet give reliable and accurate predictions at higher nuclear densities. We note that there have been efforts to improve the convergence of many-body calculations by rearranging the chiral effective field theory expansion at nonzero density [15,16]. If one reaches high enough orders in the χEFT expansion, then the systematic errors will eventually decrease as more and more low-energy parameters are tuned to empirical data. However, the predictive power of the *ab initio* approach will be diminished as more data will be needed to constrain the higher-body forces. Furthermore, the computational effort will increase significantly to the point where a first principles treatment may not be practical.

One pragmatic approach is to further constrain the nuclear force using nuclear structure data from medium mass nuclei or the saturation properties of nuclear matter [14]. This approach has been applied successfully in several recent calculations [17–20]. A rather different line of investigation has looked at the microscopic origins of the problem. In Ref. [21] numerical evidence is shown that nuclear matter sits near a quantum phase transition between a Bose gas of alpha particles and nuclear liquid. It is argued that local SU(4)-invariant forces play an increasingly important role at higher nuclear densities. The term local refers to velocity-independent interactions, as opposed to nonlocal interactions which are velocity dependent. The SU(4) refers to Wigner's approximate symmetry of the nuclear interactions where the four nucleonic degrees of freedom (proton spin-up, proton spin-down, neutron spin-up, neutron spin-down) can be rotated into each other [22].

The importance of SU(4)-invariant interactions can be understood in terms of coherent enhancement. Spin-dependent forces tend to cancel when summing over all possible nucleonic spin

* Corresponding author.
E-mail address: leed@frib.msu.edu (D. Lee).

https://doi.org/10.1016/j.physletb.2019.134863
0370-2693/

configurations. For example, we have seen in lattice calculations of binding energies for closed shell systems that the contribution from the repulsive P-wave channels often cancels most of the contribution from the attractive P-wave channels. We note also the intriguing analysis in Ref. [23] which demonstrates the connection between quantum chromodynamics with a large number of colors to Wigner's SU(4) symmetry for the S-wave interactions and Serber symmetry for the P-wave interactions. Similarly most isospin-dependent forces tend to cancel in symmetric nuclear matter due to the equal number of protons and neutrons, the one notable exception being the Coulomb interaction. The idea of SU(4) universality at large S-wave scattering length has a rich history in nuclear physics. It is well known that the Tjon line relating ^{3}H and ^{4}He binding energies is a manifestation of universality in nuclear systems [24,25]. It has also been shown that ^{3}H and ^{4}He are characterized by universal physics associated with the Efimov effect [26,27]. The coherent enhancement of SU(4)-invariant forces in the nuclear many-body environment suggests a possible resurgence of SU(4) symmetry in heavier nuclei as well. This idea inspired the exploratory work in Ref. [28] on the structure of nuclei up through oxygen using an SU(4)-invariant interaction. This built upon previous work in Ref. [21] which showed that local SU(4)-invariant interactions have a particularly strong effect on nuclear binding. The special role of local forces has also been studied by looking at the effective interactions between two bound dimers in a one-dimensional model [29].

In this work we attempt to tie all of the loose threads together. We start by acknowledging that not every χEFT interaction will give well controlled and reliable results for heavier systems. Additional ingredients are needed to make sure that the convergence of higher-order terms is under control. In order to see what the essential elements might be, we take a constructive reductionist approach and deduce the minimal nuclear interaction that can reproduce the ground state properties of light nuclei, medium-mass nuclei, and neutron matter simultaneously with no more than a few percent error in the energies and charge radii.

We start with a simple SU(4)-invariant leading order effective field theory without explicit pions (pion-less EFT) on a periodic L^3 cube with lattice coordinates $\boldsymbol{n} = (n_x, n_y, n_z)$. The Hamiltonian is

$$H_{\mathrm{SU}(4)} = H_{\mathrm{free}} + \frac{1}{2!}C_2 \sum_{\boldsymbol{n}} \tilde{\rho}(\boldsymbol{n})^2 + \frac{1}{3!}C_3 \sum_{\boldsymbol{n}} \tilde{\rho}(\boldsymbol{n})^3, \tag{1}$$

where H_{free} is the free nucleon Hamiltonian with nucleon mass $m = 938.9$ MeV. The density operator $\tilde{\rho}(\boldsymbol{n})$ is defined in the same manner as in Ref. [28],

$$\tilde{\rho}(\boldsymbol{n}) = \sum_i \tilde{a}_i^\dagger(\boldsymbol{n})\tilde{a}_i(\boldsymbol{n}) + s_L \sum_{|\boldsymbol{n}'-\boldsymbol{n}|=1} \sum_i \tilde{a}_i^\dagger(\boldsymbol{n}')\tilde{a}_i(\boldsymbol{n}'), \tag{2}$$

where i is the joint spin-isospin index and the smeared annihilation and creation operators are defined as

$$\tilde{a}_i(\boldsymbol{n}) = a_i(\boldsymbol{n}) + s_{NL} \sum_{|\boldsymbol{n}'-\boldsymbol{n}|=1} a_i(\boldsymbol{n}'). \tag{3}$$

The summation over the spin and isospin implies that the interaction is SU(4) invariant. The parameter s_L controls the range of the local part of the interaction, while s_{NL} controls the range of the nonlocal part of the interaction. The parameters C_2 and C_3 give the strength of the two-body and three-body interactions, respectively.

In this letter we use a lattice spacing $a = 1.32$ fm, which corresponds to a momentum cutoff $\Lambda = \pi/a \approx 465$ MeV. The dynamics with momentum Q much smaller than Λ can be well described and residual lattice artifacts are suppressed by powers of Q/Λ [30]. In Ref. [31] we showed that the nucleon-nucleon scattering phase shift can be precisely extracted on the lattice using the spherical wall method. In this work we fix the two-body interaction by fitting the scattering length a_0 and effective range r_0. In each instance we calculate the S-wave phase shifts below relative momentum $P_{\mathrm{rel}} \le 50$ MeV using the spherical wall method and calculate fit errors by comparing results with the effective range expansion.

For systems with more than three nucleons, we use auxiliary-field Monte Carlo lattice simulations for a cubic periodic box with length L [32,33]. For nuclei with $A < 30$ nucleons, we take $L \ge 8$, with larger values of L for cases where more accuracy is desired. For nuclei with $A \ge 30$ we take $L = 9$. The temporal lattice spacing is 0.001 MeV^{-1} and the projection time is set to 0.3 MeV^{-1}. We find that these settings are enough to provide accurate results for systems with $A \le 48$. We also use the recently-developed pinhole algorithm [28] in order to calculate density distributions and charge radii.

We use few-body data with $A \le 3$ to fix the interaction coefficients C_2 and C_3, while the range of the interactions are controlled by the parameters s_{NL} and s_L. The particular combination of s_{NL} and s_L we choose is set through a procedure we now describe. In the few-body sector, the two smearing parameters s_{NL} and s_L produce very similar effects and are difficult to distinguish from few-body data alone [21]. Therefore the chosen values for s_{NL} and s_L are fixed later after calculating heavier nuclei. The two-body interaction strength C_2 and interaction range are determined by fitting the scattering length a_0 and effective range r_0 averaged over the two S-wave channels, $^1S_0$ and $^3S_1$. We adjust a_0 to minimize the corrections to the ^{3}H and ^{4}He binding energies that arise from the differences between the two S-wave channels. This process gives an optimal value of $a_0 = 9.1$ fm, and we use this value for a_0 in what follows. We note that our SU(4)-invariant deuteron is degenerate with the di-neutron ground state and has less than half of the physical deuteron binding energy. However this issue is easily fixed when SU(4)-breaking interactions are included. For the SU(4)-averaged effective range we use $r_0 = (r_0(^1S_0) + r_0(^3S_1))/2 \approx$ 2.2 fm.

We determine the three-body coupling strength C_3 by fitting to the ^{3}H binding energy. At the physical point $B(^3\mathrm{H}) = 8.48$ MeV, the ^{4}He binding energy with the Coulomb interaction included is 28.9 MeV. This is close to the experimental value $B(^4\mathrm{He}) =$ 28.3 MeV. We carry out this fitting process for several different pairs of values for s_{NL} and s_L, and for each pair we calculate a handful of nuclear ground states using auxiliary-field lattice Monte Carlo simulations. As described in the Supporting Online Materials section, we find that the pair $s_{NL} = 0.5$ and $s_L = 0.061$ gives the best overall description. The full set of optimized parameters are $C_2 = -3.41 \times 10^{-7}$ MeV^{-2}, $C_3 = -1.4 \times 10^{-14}$ MeV^{-5}, $s_{NL} = 0.5$, and $s_L = 0.061$.

In Table 1 we show the binding energies and charge radii for selected nuclei. For comparison we also list the experimental values and the calculated Coulomb energy. While the ^{3}H energy is exact due to the fitting procedure, all the other values are predictions. The largest relative error in binding energy is 4% and occurs for ^{16}O. The largest relative error in the charge radius is 8% and occurs for ^{3}H. For the calculations of nuclear charge radii, we have taken into account the charge radius of the proton.

We now calculate the binding energies for 86 bound even-even nuclei (even number of protons, even number of neutrons) with up to $A = 48$ nucleons. The results are shown and compared with empirical data in Fig. 1. Because the interaction has an exact SU(4) symmetry, we are free of the sign problem and can calculate the binding energies with high precision. In Fig. 1 all of the Monte Carlo error bars are smaller than the size of the symbols. The re-

Table 1
Comparison of calculations and experiments for selected nuclei. The calculated binding energies and charge radii of ^{3}H, ^{3}He and selected alpha-like nuclei compared with experimental values. The Coulomb interaction is taken into account perturbatively. The first and second parentheses denote the Monte Carlo error and time extrapolation error, respectively. All energies are in MeV and all radii in fm. Experimental binding energies are taken from Ref. [34] and radii from Ref. [35].

	B	Exp.	Coulomb	B/Exp.	R_{ch}	Exp.	R_{ch}/Exp.
^{3}H	8.48(2)(0)	8.48	0.0	1.00	1.90(1)(1)	1.76	1.08
^{3}He	7.75(2)(0)	7.72	0.73(1)(0)	1.00	1.99(1)(1)	1.97	1.01
^{4}He	28.89(1)(1)	28.3	0.80(1)(1)	1.02	1.72(1)(3)	1.68	1.02
^{16}O	121.9(1)(3)	127.6	13.9(1)(2)	0.96	2.74(1)(1)	2.70	1.01
^{20}Ne	161.6(1)(1)	160.6	20.2(1)(1)	1.01	2.95(1)(1)	3.01	0.98
^{24}Mg	193.5(02)(17)	198.3	28.0(1)(2)	0.98	3.13(1)(2)	3.06	1.02
^{28}Si	235.8(04)(17)	236.5	37.1(2)(3)	1.00	3.26(1)(1)	3.12	1.04
^{40}Ca	346.8(6)(5)	342.1	71.7(4)(4)	1.01	3.42(1)(3)	3.48	0.98

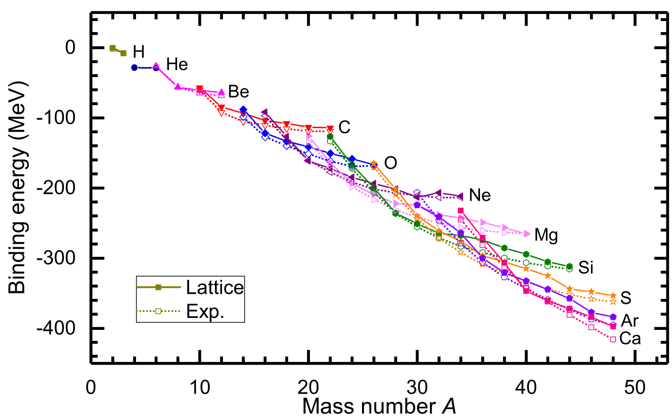

Fig. 1. Nuclear binding energies. The calculated binding energies from ^{3}H to ^{48}Ca. The solid symbols denote the lattice results and the open symbols denote the experimental values. Different symbols and colors denote different element. The Coulomb interaction is taken into account perturbatively. The experimental values are taken from Ref. [34].

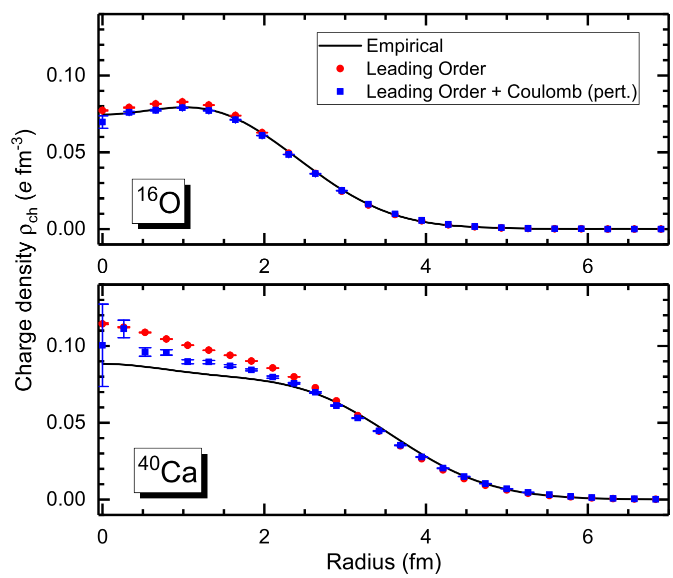

Fig. 2. Charge density distributions. The calculated ^{16}O and ^{40}Ca charge densities compared with the empirical results. The circles denote the results without Coulomb interaction. The squares denote the results with the Coulomb interaction included perturbatively. Empirical values are taken from Ref. [36].

maining errors due to imaginary time and volume extrapolations are also small, less than 1% relative error, and thus are also not explicitly shown. In Fig. 1 we see that the general trends for the binding energies along each isotopic chain are well reproduced. In particular, the isotopic curves on the proton-rich side are close to the experimental results. The discrepancy is somewhat larger on the neutron-rich side and is a sign of missing effects such as spin-dependent interactions.

The charge density profile is another important probe of nuclear structure. In Fig. 2 we show the charge densities of ^{16}O and ^{40}Ca calculated with the pinhole algorithm. We have again taken into account the charge distribution of the proton. To compare with data from the electron scattering experiments we also show results with the Coulomb interaction included via first order perturbation theory. The Coulomb force suppresses the central densities, drawing the results closer to the empirical data. Our results are quite accurate for such a simple nuclear interaction.

We also examine the predictions for pure neutron matter (NM). In Fig. 3 we show the calculated NM energy as a function of the neutron density and the comparison with other calculations using next-to-next-to-next-to-leading-order (N^{3}LO) chiral interactions. In the lattice results we vary the number of neutrons from 14 to 66. The data for three different box sizes L=5 (upright triangles), L=6 (squares), L=7 (rightward-pointing triangles) are marked as filled red polygons. We see that our results are in general agreement with the other calculations at densities above 0.05 fm^{-3}, though calculations at higher orders are needed and are planned in future work to estimate uncertainties. At lower densities the discrepancy is larger as a result of our SU(4)-invariant interaction having the incorrect neutron-neutron scattering length. The open red polygons, again L=5 (upright triangles), L=6 (squares), L=7 (rightward-pointing triangles), show an improved calculation with a short-range interaction to reproduce the physical neutron-neutron scattering length as well as a correction to improve invariance under Galilean boosts. The restoration of Galilean invariance on the lattice is described in Ref. [40]. Overall, the results are quite good in view of the simplicity of the four-parameter interaction.

In this letter we have shown that the ground state properties of light nuclei, medium-mass nuclei, and neutron matter can be described using a minimal nuclear interaction with only four interaction parameters. While the first three parameters are already standard in χEFT, the fourth and last parameter is a new feature that controls the strength of the local part of the nuclear interactions. These insights can help design χEFT interactions with better convergence at higher densities. We encourage others to test simplified interactions in continuum nuclear structure calculations, interactions with SU(4) symmetry and a combination of local and nonlocal smearing. The details of our interaction are given in the Supplemental Material. In the continuum calculations, however, one can construct interactions with exact Galilean invariance, something that needs to be corrected order by order on the lattice [40].

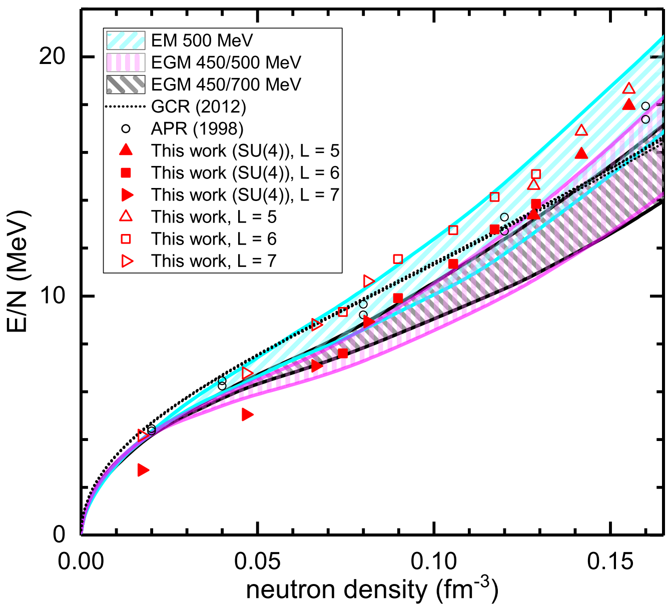

Fig. 3. Pure neutron matter. The pure neutron matter (NM) energy as a function of neutron density calculated using the NL50 interaction with box size L=5 (upright triangles), L=6 (squares), L=7 (rightward-pointing triangles), respectively. The filled red polygons show results for the leading-order SU(4)-symmetric interaction. The open red polygons show an improved calculation with a short-range interaction to reproduce the physical neutron-neutron scattering length as well as a correction to improve invariance under Galilean boosts. For comparison we also show results calculated with full N^{3}LO chiral interactions (EM 500 MeV, EGM 450/500 MeV and EGM 450/700 MeV) [37], the results from variational (APR) [38] and Auxiliary Field Diffusion MC calculations (GCR) [39].

We are now using SU(4)-symmetric short-range interactions with local and nonlocal smearing and also one-pion exchange as the starting point for improved calculations of light and medium-mass nuclei with chiral forces up to N^{3}LO. While our ongoing N^{3}LO work is far from finished, we do know that the corrections at NLO are typically at the 10% level in the binding energies. We should clarify that what we called LO in lattice chiral effective field theory is actually an improved LO calculation where the S-wave effective range correction is included. If the S-wave effective range correction were not included at LO, then the NLO correction would be at the 30% level. This 10% correction at NLO might still seem too large since the agreement between the LO results in this work and the experimental binding energies are better than 10%. However, this better-than-expected agreement can be explained by the additional fine-tuning we gain by adjusting the balance between local and nonlocal interactions to achieve accurate liquid drop properties.

The main takeaway message of the work presented here is that while some fine tuning of the chiral forces seems necessary to improve convergence at higher densities, the number of independent fine tunings does not appear to be large. While we have not solved the convergence problem, we characterized the scope of problem. The key remaining question is how to accomplish these fine tunings without fitting to the many-body data that we wish to predict. We plan to address this question in a forthcoming publication.

Aside from the Coulomb interaction, all of the other interactions in our minimal model respect Wigner's SU(4) symmetry. This is an example of emergent symmetry. The SU(4)-invariant interaction resurges at higher densities not because the underlying fundamental interaction is exactly invariant, but because the SU(4)-invariant interaction is coherently enhanced in the many-body environment. This is not to minimize the important role of spin-dependent effects such as spin-orbit couplings and tensor forces. However, it does seem to suggest that SU(4) invariance plays a key role in the bulk properties of nuclear matter.

The computational effort needed for the auxiliary-field lattice Monte Carlo simulations scales with the number of nucleons, A, as somewhere between A^1 to A^2 for medium mass nuclei. The actual exponent depends on the architecture of the computing platform. The SU(4)-invariant interaction provides an enormous computational advantage by removing sign oscillations from the lattice Monte Carlo simulations for any even-even nucleus. Coulomb interactions and all other corrections can be implemented using perturbation theory or the recently-developed eigenvector continuation method if the corrections are too large for perturbation theory [41]. Given the mild scaling with nucleon number and suppression of sign oscillations, the methods presented here provide a new route to realistic lattice simulations of heavy nuclei in the future with as many as one or two hundred nucleons. By realistic calculations we mean calculations where one can demonstrate order-by-order convergence in the chiral expansion going from LO to NLO, NLO to N^{2}LO, and N^{2}LO to N^{3}LO, while maintaining agreement with empirical data.

Acknowledgements

We thank A. Schwenk for providing the neutron matter results for comparison. We acknowledge partial financial support from the Deutsche Forschungsgemeinschaft (TRR 110, “Symmetries and the Emergence of Structure in QCD”), the BMBF (Grant No. 05P15PCFN1), the U.S. Department of Energy (DE-SC0018638 and DE-AC52-06NA25396), and the Scientific and Technological Research Council of Turkey (TUBITAK project No. 116F400). Further support was provided by the Chinese Academy of Sciences (CAS) President's International Fellowship Initiative (PIFI) (grant No. 2018DM0034) and by VolkswagenStiftung (grant No. 93562). The computational resources were provided by the Julich Supercomputing Centre at Forschungszentrum Jülich, Oak Ridge Leadership Computing Facility, RWTH Aachen, and Michigan State University.

Appendix A. Supplementary material

Supplementary material related to this article can be found online at https://doi.org/10.1016/j.physletb.2019.134863.

References

[1] E. Epelbaum, H.W. Hammer, U.-G. Meißner, Rev. Mod. Phys. 81 (2009) 1773.
[2] R. Machleidt, D.R. Entem, Phys. Rep. 503 (2011) 1.
[3] G. Hupin, S. Quaglioni, P. Navrátil, Phys. Rev. Lett. 114 (21) (2015) 212502.
[4] P. Navrátil, V.G. Gueorguiev, J.P. Vary, W.E. Ormand, A. Nogga, S. Quaglioni, Few-Body Syst. 43 (2008) 129.
[5] D. Lonardoni, J. Carlson, S. Gandolfi, J.E. Lynn, K.E. Schmidt, A. Schwenk, X. Wang, Phys. Rev. Lett. 120 (12) (2018) 122502.
[6] M. Piarulli, et al., Phys. Rev. Lett. 120 (5) (2018) 052503.
[7] E. Epelbaum, et al., LENPIC Collaboration, Phys. Rev. C 99 (2) (2019) 024313.
[8] M. Wloch, D.J. Dean, J.R. Gour, M. Hjorth-Jensen, K. Kowalski, T. Papenbrock, P. Piecuch, Phys. Rev. Lett. 94 (2005) 212501.
[9] G. Hagen, T. Papenbrock, D.J. Dean, M. Hjorth-Jensen, Phys. Rev. Lett. 101 (2008) 092502.
[10] G. Hagen, M. Hjorth-Jensen, G.R. Jansen, R. Machleidt, T. Papenbrock, Phys. Rev. Lett. 108 (2012) 242501.
[11] S. Binder, J. Langhammer, A. Calci, R. Roth, Phys. Lett. B 736 (2014) 119.
[12] E. Epelbaum, H. Krebs, T.A. Lähde, D. Lee, U.-G. Meißner, G. Rupak, Phys. Rev. Lett. 112 (10) (2014) 102501.
[13] A. Cipollone, C. Barbieri, P. Navrátil, Phys. Rev. C 92 (1) (2015) 014306.
[14] A. Ekström, et al., Phys. Rev. C 91 (5) (2015) 051301, https://doi.org/10.1103/PhysRevC.91.051301, arXiv:1502.04682 [nucl-th].
[15] U.-G. Meißner, J.A. Oller, A. Wirzba, Ann. Phys. 297 (2002) 27.
[16] A. Lacour, J.A. Oller, U.-G. Meißner, Ann. Phys. 326 (2011) 241.
[17] G. Hagen, et al., Nat. Phys. 12 (2) (2015) 186.

[18] G. Hagen, G.R. Jansen, T. Papenbrock, Phys. Rev. Lett. 117 (17) (2016) 172501.
[19] J. Simonis, S.R. Stroberg, K. Hebeler, J.D. Holt, A. Schwenk, Phys. Rev. C 96 (1) (2017) 014303.
[20] T.D. Morris, et al., Phys. Rev. Lett. 120 (15) (2018) 152503.
[21] S. Elhatisari, et al., Phys. Rev. Lett. 117 (13) (2016) 132501.
[22] E. Wigner, Phys. Rev. 51 (1937) 106.
[23] A. Calle Cordon, E. Ruiz Arriola, Phys. Rev. C 80 (2009) 014002, https://doi.org/10.1103/PhysRevC.80.014002, arXiv:0904.0421 [nucl-th].
[24] L. Platter, H.-W. Hammer, U.-G. Meißner, Phys. Lett. B 607 (2005) 254, https://doi.org/10.1016/j.physletb.2004.12.068, arXiv:nucl-th/0409040.
[25] N. Klein, S. Elhatisari, T.A. Lähde, D. Lee, U.-G. Meißner, Eur. Phys. J. A 54 (7) (2018) 121.
[26] S. König, H.W. Grießhammer, H.W. Hammer, U. van Kolck, Phys. Rev. Lett. 118 (20) (2017) 202501.
[27] A. Kievsky, M. Gattobigio, Few-Body Syst. 57 (3) (2016) 217.
[28] S. Elhatisari, et al., Phys. Rev. Lett. 119 (22) (2017) 222505.
[29] A. Rokash, E. Epelbaum, H. Krebs, D. Lee, Phys. Rev. Lett. 118 (23) (2017) 232502.
[30] N. Klein, D. Lee, U.-G. Meißner, Eur. Phys. J. A 54 (12) (2018) 233.
[31] B.N. Lu, T.A. Lähde, D. Lee, U.-G. Meißner, Phys. Lett. B 760 (2016) 309.
[32] D. Lee, Prog. Part. Nucl. Phys. 63 (2009) 117.
[33] T.A. Lähde, U.-G. Meißner, Lect. Notes Phys. 957 (2019) 1.
[34] M. Wang, et al., Chin. Phys. C 41 (2017) 030003.
[35] I. Angeli, K.P. Marinova, At. Data Nucl. Data Tables 99 (1) (2013) 69.
[36] H. De Vries, C.W. De Jager, C. De Vries, At. Data Nucl. Data Tables 36 (1987) 495.
[37] I. Tews, T. Krüger, K. Hebeler, A. Schwenk, Phys. Rev. Lett. 110 (3) (2013) 032504.
[38] A. Akmal, V.R. Pandharipande, D.G. Ravenhall, Phys. Rev. C 58 (1998) 1804.
[39] S. Gandolfi, J. Carlson, S. Reddy, Phys. Rev. C 85 (2012) 032801.
[40] N. Li, S. Elhatisari, E. Epelbaum, D. Lee, B. Lu, U.G. Meißner, Phys. Rev. C 99 (6) (2019) 064001.
[41] D. Frame, R. He, I. Ipsen, D. Lee, D. Lee, E. Rrapaj, Phys. Rev. Lett. 121 (3) (2018) 032501.